Queen Mary
University of London

Background Subtraction with Dirichlet Process Mixture Models.

Haines, TS; Xiang, T

For additional information about this publication click this link.
http://qmro.qmul.ac.uk/xmlui/handle/123456789/11343

Information about this research object was correct at the time of download; we occasionally make corrections to records, please therefore check the published record when citing. For more information contact scholarlycommunications@qmul.ac.uk

Background Subtraction with Dirichlet Process Mixture Models

Tom S. F. Haines and Tao Xiang

Abstract—Video analysis often begins with background subtraction. This problem is often approached in two steps - a background model followed by a regularisation scheme. A model of the background allows it to be distinguished on a per-pixel basis from the foreground, whilst the regularisation combines information from adjacent pixels. We present a new method based on Dirichlet process Gaussian mixture models, which are used to estimate per-pixel background distributions. It is followed by probabilistic regularisation. Using a non-parametric Bayesian method allows per-pixel mode counts to be automatically inferred, avoiding over-/under- fitting. We also develop novel model learning algorithms for continuous update of the model in a principled fashion as the scene changes. These key advantages enable us to outperform the state-of-the-art alternatives on four benchmarks.

Index Terms—Background subtraction, Dirichlet processes, non-parametric Bayesian methods, confidence capping, video analysis

1 Introduction

Background subtraction can be defined as a binary segmentation of a video stream, into the foreground, which is unique to a particular moment in time, and the background, which is always present. It is typically used as an interest detector for higher level problems, such as automated surveillance, action recognition, intelligent environments and motion analysis. The etymology of *background subtraction* derives from the original approach, where a single static image of just the background is subtracted from the current frame, to generate a difference image. If the absolute difference exceeds a threshold the pixel in question is declared to belong to the foreground. This approach performs poorly because it assumes a static background with well behaved objects - in practise this is almost never the case. Many situations break these assumptions [1], [2]:

Dynamic background, where objects such as trees blow in the wind, escalators move and traffic lights change colour. These objects, whilst moving, still belong to the background as they are of no interest to further analysis.

Noise, as caused by the image capturing process. It can vary over the image due to photon noise and varying brightness. In some cases, such as low light/thermal, it can dominate.

Camouflage, where a foreground object looks very much like the background, e.g. a sniper in a ghillie suit.

Camera shake often exists, a symptom of mount points that are subject to wind or vibrations. This can be considered to be a type of highly correlated global noise.

Moved object (class transitions), where the foreground becomes part of the background, or vice versa; e.g. a car could be parked in the scene, and after sufficient time considered part of the background, only to later become foreground again when driven off.

Bootstrapping. As it is often not possible to get a frame with no foreground an algorithm should be capable of being initialised with foreground objects in the scene. It has to then learn the correct background model over time.

Shadows are cast by the foreground objects, but later processing is typically not interested in them.

Illumination changes, both gradual, e.g. from the sun moving during the day, and rapid, such as from a light switch being toggled.

Addressing these challenges, particularly the first three, leads to a number of considerations in designing a background model. Specifically, on account of the *dynamic* nature of backgrounds the model has to classify a range of pixels as belonging to the background. This can be represented with a multi-modal distribution, e.g. a tree waving against the sky generates pixels that are sky one moment and tree another, but both sets need to modelled as background. How many modes exist will need to be learnt, and can potentially change with time, e.g. a windy day versus a calm day. *Noise* is generated by both the image capture process and typical small scale variations in the background colour. It is primarily modelled using the variance of a probability distribution, which needs to be set high enough to capture the variation. *Camouflage* on the other hand is when a foreground object looks like it belongs to the background, either deliberately or accidentally. The effect of camouflage is interleaved with that of noise: noise can increase the range of values considered to belong to the background, allowing a camouflaged object to remain undetected. Consequentially the variance of the background representation is a trade-off - too low and

- *T. S. F. Haines is with the Department of Computer Science, University College London, Gower Street, London WC1E 6BT*
E-mail: thaines@cs.ucl.ac.uk
- *T. Xiang is with the School of Electronic Engineering and Computer Science, Queen Mary, University of London, Mile End Road, London E1 4NS*
E-mail: txiang@eecs.qmul.ac.uk
- *Both authors are funded by EPSRC under the EP/G063974/1 grant.*

noise will trigger detection; too high and camouflaged objects will be missed. Variance therefore needs to be learnt from the data. Noting that as noise can vary with both location and time (e.g. photon noise only matters in the dark areas of an image, at night.), this needs to be continuously calculated from the video feed, on a per-region basis. A desirable background model thus should learn the number of modes required to represent the background, including the variance of each mode, such that it handles noise without compromising its ability to detect camouflaged entities.

To this end we propose to use a *Dirichlet process Gaussian mixture model* (DP-GMM) [3] to provide a per-pixel density estimate. This is a non-parametric Bayesian method [4] that automatically estimates the number of mixture components required to model the pixels background colour distribution, e.g. a tree waving backwards and forward in front of the sky will generate single mode pixels at the trunk and in the sky, but two mode pixels in the area where the branches wave, such that the pixels transition between leaf and sky regularly. If it needs more modes to represent multiple leaf colours this will occur automatically, and, of great importance for long term surveillance, the model will update with time as new evidence becomes available, e.g. on a calm day when the tree is not moving it will revert to single mode pixels throughout. As it is fully Bayesian it avoids over-/under- fitting its model.

However, there are two issues that prevent a standard DP-GMM from being used as a per-pixel background model: 1) the existing model update techniques cannot cope with the scene changes common in real-world applications; 2) using the model for continuous video streams is unscalable both in terms of memory usage and computational cost. To solve the first issue and make the DP-GMM suitable for background modelling, a set of novel model update techniques are developed in this work. More specifically, each mode in the model represents a range of colours, using a Gaussian distribution[1]. The extent of this range is learnt from the data stream, and is again updated as the scene changes. During the day when pixels are almost constant it will select a tight distribution, whilst at night it will expand as photon noise pushes the range of expected values wider. A visual scene typically evolves as time goes by, e.g. the day/night cycle, a car parking, road works remodelling a traffic junctions layout, with different speeds of change. Consequentially the model needs to *forget* what it has previously learnt and model the new background effectively and efficiently. For this we introduce a novel model update concept that lets old information degrade in a principled way, which we refer to as *confidence capping*. It limits how confident it can be about any given mode, which puts a constraint on how certain it can be about the shape of the background distribution. As a result, when a mode is no longer used it will slowly fade away, whilst the new mode(s) start to dominate the model. If during this period the scene reverts to the old state it can start using its old modes again. This allows a stationary object to remain part of the foreground for a long time, as it takes a lot of information for the new component to obtain the confidence of pre-existing components, but when an object moves on and the background changes to a component it has seen before, even if a while ago, it can use that component immediately. Updating the components for gradual background changes (e.g. gradual *illumination changes*) continues to happen, making sure the model is never left behind by gradual changes. This also helps with *bootstrap* performance, as it can quickly learn the model, even with foreground objects.

To overcome the second issue on model scalability, two measures are taken. First, we fit the model by Gibbs sampling each sample only once. This would normally compromise model convergence, but because of confidence capping and the availability of a never ending stream of data the model will converge regardless. In addition to its computational saving it avoids the need to store and process hundreds of previous video frames, which can consume vast amount of memory [1], [5]. This memory consumption problem is particularly noticeable for approaches based on kernel density estimation [6], [7], [8], [9], [10]. Second, to obtain real time performance, we introduce a GPU based implementation.

To summarise the contributions are: 1) a new background subtraction technique is proposed [11] built on a non-parametric Bayesian density estimate, which avoids over-/under- fitting; 2) A novel model update is formulated that is both principled and practical - the approach is real time with a constant memory requirement; 3) An exhaustive evaluation using four data sets [1], [2], [12], [13] demonstrates top performance in comparison with the state-of-the-art alternatives. The code, both a C version and a GPU version, has been made available[2].

1.1 Related Work

The background subtraction field is humongous, and has many review papers [2], [14], [15], [16]. Stauffer & Grimson [17] is one of the best known approaches - it uses a Gaussian mixture model (GMM) for a per-pixel density estimate (DE) followed by connected components for regularisation. This model improves on using a background plate because it can handle a *dynamic background* and *noise*, by using multimodal probability distributions. As it is continuously updated it can *bootstrap*. Its mixture model includes both foreground and background components - it classifies values based on their mixture component, which is assigned to the foreground or the background based on the assumption that the majority of the larger components belong to the background, with the remainder foreground. This

1. This is actually integrated out, such that a student-t distribution is used in practise.

2. Accessible at http://www.thaines.com

assumption fails if objects hang around for very long, as they quickly dominate the distribution. It has a fixed component count, which does not match real variability, where the number of modes differs between pixels. The model is updated linearly using a fixed learning rate parameter - consequentially the *moved object* problem is an unhelpful trade between ghosting and forgetting stationary objects too quickly. Connected components converts the intermediate foreground mask into regions via pixel adjacency, and culls all regions below a certain size, to remove spurious detections. This approach to noise handling combined with its somewhat primitive density estimation method undermines *camouflage* handling, as it often thinks it is noise, and also prevents it from tracking small objects. No capacity exists for it to handle *illumination changes* or *shadows*. The above can be divided into four parts - the model, updating the model, how pixels are classified, and regularisation; alternative approaches for each will now be considered in turn.

The model: Alternative DE methods exist, including different GMM implementations [9] and kernel density estimate (KDE) methods, either using Gaussian kernels [6], [7] or step kernels [8], [9], [10]. Histograms have also been used [18], and alternatives to DE include models that predict the next value [1], use neural networks [19], [20], [21], or hidden Markov models [22]. Alternatives to the GMM background model can improve handling of *dynamic background*, *noise* and *camouflage* by better reflecting the underlying variability of the background. This can be particularly important with relation to over-/under- fitting, as the model needs to accurately generalise the data stream. All models suffer from some degree of over-/under- fitting. KDE and histogram methods are particularly vulnerable, as they implicitly assume a constant density by using fixed size kernels/bins. GMM methods should do better, but the heuristics required for online learning, particularly regarding the creation of new components, can result in local minima in the optimisation, which is just as problematic. He et al. [5] recently used DP-GMMs for background subtraction, in common with the presented approach. They failed to leverage the potential advantages however (discussed below), and used computationally unscalable methods. It is block-based, which is to say they ran the model at very low resolution to save computation, and it has unbounded memory consumption. Consequentially it is not applicable to real world scenarios, and, despite their efforts, poor results were obtained. Global models should in principal be better, with techniques based on principal component analysis (PCA) [23] having shown the most promise. They attempt to model the background as a low dimensional subspace of the vectorised input, with the foreground identified as outliers. In practise such approaches have struggled, due to high computational requirements and limited capability to deal with many common problems, e.g. camouflage. They tend to excel at camera shake however, and recent variants have resolved many of the issues [24], [25].

Model update: Most methods use a constant learning rate to update the model, but some use adaptive heuristics [9], [10], [26], whilst others are history based [1], [5], [10], and build a model from the last n frames directly. Adapting the learning rate affects the *moved object* issue - if it is too fast then stationary objects become part of the background too quickly, if it is too slow it takes too long to recover from changes to the background. Adaptation aims to adjust the rate depending on what is happening. There is invariably a trade-off between quickly learning when the background model has changed and accepting foreground objects into the background when they stop moving for a while (cars at traffic lights.) - trying to minimise this trade-off is a key goal and no perfect solution exists. In addition continuously learning the model is required to handle the *bootstrapping* issue. We present confidence capping (see above), which works because non-parametric Bayesian models, such as DP-GMMs, have a rigorous concept of a new mixture component forming. Parametric models [9], [17] have to use heuristics to simulate this, whilst a confidence cap is not possible for KDE based approaches [6], [7], [8], [9], [10] as they lack a measure of confidence.

Pixel classification: The use of a single density estimate that includes both foreground (fg) and background (bg), as done by Stauffer & Grimson [17] is somewhat unusual - most methods stick to separate models and apply Bayes rule [18], with the foreground model set to be the uniform distribution as it is unknown. We follow this convention, which results in a probability of being *bg* or *fg*, rather than a hard classification, which is passed through to the regularisation step. Instead of using Bayes rule some works use a threshold [6], [10], which can by dynamically learnt [10]. Attempts at learning a foreground model also exist [7], and some models generate a binary classification directly [19], [20], [21].

Regularisation: Some approaches have no regularisation step [27], others have information sharing between adjacent pixels [19], [20], [21] but no explicit regularisation. Techniques such as eroding then dilating are common [2], and more advanced techniques have, for instance, tried to match pixels against neighbouring pixels, to compensate for background motion [6]. When dealing with a probabilistic fg/bg assignment probabilistic methods should be used, such as the use of Markov random fields (MRF) by Migdal & Grimson [28], Sheikh & Shah [7] and Schick et al. [29]. We also use a MRF - the pixels all have a random variable which can take on one of two labels, *fg* or *bg*. The data term is provided by the model whilst pairwise potentials encourage adjacent pixels to share the same label. Differences exist - previous works use Gibbs sampling [28] and graph cuts [7], [29], whilst we choose loopy belief propagation [30], as run time can be capped, and also accelerated with a GPU implementation. We also use an edge preserving cost between pixels, rather than a constant cost, which proves to be beneficial with high levels of noise. Cohen [31] has also used a

Algorithm 1 Pseudo code for core algorithm
(Actual code available from http://www.thaines.com)

```
for frame in video:
  frame = colour_convert(frame) # Subsection 2.4 &
      supplementary material.

  model.update_global_prior(frame) # Subsection 2.4
  model.correct_lighting(frame) # Subsection 2.4

  for x,y in frame.coordinates():
    pixel = frame[x,y]
    pixel_sd = camera_shake(frame, x, y) # Eqn. 17

    for t in [components] + [new]:
      p_com[x,y,t] = model.p_draw_from_component(
          pixel, t) # Equation 9
    p_bg[x,y] = sum(p_com[x,y,:]) / 3.0 # Equation
        12 with P(bg)=0.5

    t = draw(p_com[x,y,:]) # Weighted draw
    model.update(x,y,t) # Equations 4 - 6 & 16
    model.cap_confidence(x,y) # End of subsection 2.1

  p_bg = belief_propagation(p_bg) # Regularisation,
      subsection 2.2
  mask = threshold(p_bg)
```

Markov random field, to generate a background image by selecting pixels from a frame sequence, rather than for regularisation. Parks & Fels [32] provide a review of regularisation for background subtraction.

Input: The vast majority of approaches, including this one [11], use the colours of the individual pixels directly. Other approaches use alternative information sources however, including optical flow [33], depth [34], tracking [35] and object detection [35]. Additionally, only foreground/background classification is provided by the presented approach - other approaches may mark areas as being in shadow [6], [35] or use other labelling strategies [33].

2 Methodology

The presented method naturally splits into two - a per pixel background model and a regularisation step. The GPU implementation and further details are also given. For an overview of the system Figure 1 gives a block diagram, whilst Algorithm 1 gives pseudo code of the core structure.

2.1 Per-pixel Background Model

Each pixel has its own multi-modal density estimate, used to model $P(\mathbf{x}|\text{bg})$ where $\mathbf{x}$ is the vector of pixel colour channels. The Dirichlet process Gaussian mixture model (DP-GMM) [3] is used. It can be viewed as the Dirichlet distribution extended to an infinite number of components, which allows it to learn the true number of mixtures required to represent the data. For each pixel a stream of values arrives, one with each frame - the model has to be continuously updated using incremental learning.

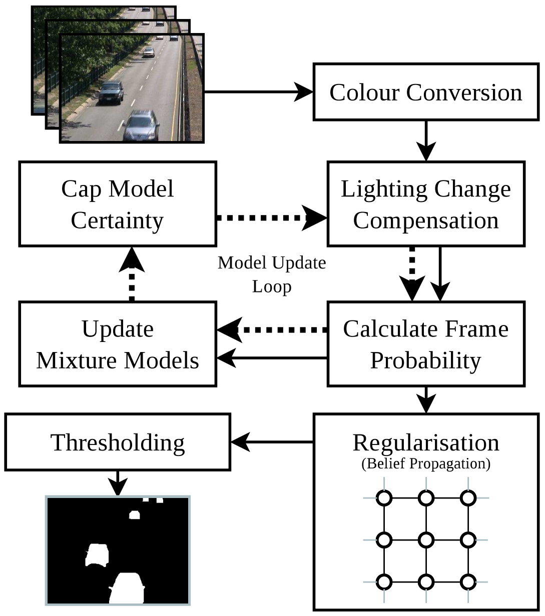

Fig. 1. Block diagram of the approach. The solid arrows show the path of a frame through the system, whilst the doted arrows show the update order of the model, which loops around for the next frame.

We start by introducing the Dirichlet process, firstly using the stick breaking construction then secondly using the Chinese restaurant process. The stick breaking construction provides a clean explanation of the concept, whilst the Chinese restaurant process integrates out irrelevant variables and provides the formulation we actually solve. Figure 2a represents the DP-GMM graphically using the *stick breaking* construction. It can be split into 3 columns - on the left the priors, in the middle the entities representing the Dirichlet process (DP) and on the right the data for which a density estimate is being constructed. This last column contains the feature vectors (pixel colours) to which the model is being fitted, $\mathbf{x}_i$, which come from all previous frames, $i \in \mathcal{I}$. It is a generative model - each sample comes from a specific mixture component, indexed by $Z_i \in \mathcal{K}$, which consists of its probability of being selected, V_k and the Gaussian distribution from which the value was drawn, η_k. The conjugate prior, consisting of μ, a Gaussian over its mean, and Λ, a Wishart distribution over its precision (inverse covariance matrix), is applied to all η_k. So far this is just a mixture model; the interesting part is that $\mathcal{K}$, the set of mixture components, is infinite. Conceptually the stick breaking construction is very simple - we have a stick of length 1, representing the entire probability mass, which we keep breaking into two parts. Each time it is broken one of the parts becomes the probability mass for a mixture component - a value of V_k, whilst the other is kept for the next break. This continues forever. α is the concentration parameter, which controls how the stick is broken - a low value puts most of the probability mass in a few mixture components, whilst a high value spreads it out over many. Stick lengths are represented by the

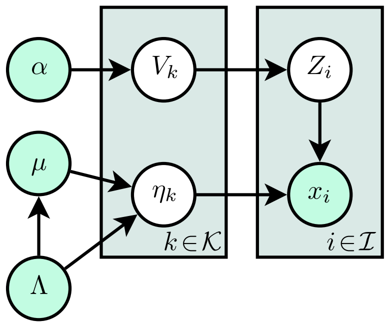

(a) Stick breaking

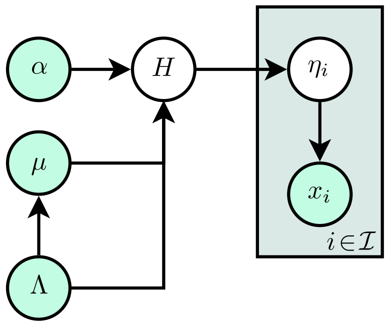

(b) Chinese restaurant

Fig. 2. Two representations of the DP-GMM graphical model, each corresponding to a specific implementation techniques.

random variable V_k, which is defined as

$$V_k = \upsilon_k \prod_{i\in[0,k)} (1-\upsilon_i), \qquad \upsilon_k \sim \mathrm{Beta}(1,\alpha) \tag{1}$$

where $\mathrm{Beta}(\cdot,\cdot)$ is the beta distribution and $k\in\mathcal{K}$ is the infinite set of sticks. In effect, the υ_k values are how much of the remaining stick to use for probability mass k, whilst V_k is the remaining stick length, calculated from the previous breaks, multiplied by the amount of the remainder to use for stick k. Orthogonal to the stick length, each stick is associated with a draw, η_k, from the DP's base measure, which is the already mentioned conjugate prior over the Gaussian.

Whilst the stick breaking construction offers a clean explanation of the model the Chinese restaurant process (CRP) is used for the implementation[3]. This is the model with the middle column of Figure 2a integrated out, to give Figure 2b. It is named by an analogy. Specifically, each sample is represented by a customer, which turns up and sits at a table in a Chinese restaurant. Tables represent the mixture components, and a customer chooses either to sit at a table where customers are already sitting, with probability proportional to the number of customers at that table, or to sit at a new table, with probability proportional to α. At each table (component) only one dish is consumed, which is chosen from the menu (base measure) by the first customer to sit at that table. Integrating out the draw from the DP leads to better convergence, but more importantly replaces the infinite set of sticks with a computationally tractable finite set of tables. Whilst the theory behind Dirichlet processes is deep, the actual implementation of a CRP is fairly trivial, as it can be treated as the addition of a dummy table, representing the creation of a new table, to an otherwise standard mixture model. Note that when the dummy table is used a new one is made available.

3. Variational methods [36] offer one approach to using the stick breaking construction directly. This is impractical however as historic pixel values would need to be kept.

The DP-GMM density estimate for each pixel is updated with each new frame. Updating proceeds by first calculating the probability of the current pixel value, $\mathbf{x}$, given the current background model, then updating the model with $\mathbf{x}$, weighted by the calculated probability - these steps are now detailed.

Mixture components: The per-pixel model is a set of weighted mixture components, such that the weights sum to 1, where each component is a Gaussian distribution. They are integrated out however, using the Chinese restaurant process for the mixture weights and the conjugate prior for the Gaussians (student-t distribution). Whilst the literature [37] already details this second part it is included for completeness. $x_i \in [0,1], i \in \{0,1,2\}$ represents the pixels colour, and independence is assumed between the components for reasons of speed (Equivalent to a covariance matrix where off diagonal entries are zero.). This simplifies the Wishart prior to a gamma prior for each channel i, such that

$$\sigma_i^{-2} \sim \Gamma\left(\frac{n_{i,0}}{2}, \frac{\sigma^2_{i,0}}{2}\right), \qquad \mu_i|\sigma_i^2 \sim \mathcal{N}\left(\mu_{i,0}, \frac{\sigma_i^2}{k_{i,0}}\right), \tag{2}$$

$$x_i \sim \mathcal{N}(\mu_i, \sigma_i^2), \tag{3}$$

where $\mathcal{N}(\mu,\sigma^2)$ represents the normal distribution and $\Gamma(\alpha,\beta)$ the gamma distribution. The parameters $n_{i,0}$ and $\sigma_{i,0}$, $i \in \{0,1,2\}$, are the Λ prior from the graphical model, whilst $\mu_{i,0}$ and $k_{i,0}$ are the μ prior.

Evidence, $\mathbf{x}$, is provided incrementally, one sample at a time, which will be weighted by w, the probability that it belongs to the background model. The model is then updated from having m samples to $m+1$ samples using

$$n_{i,m+1} = n_{i,m} + w, \tag{4}$$

$$k_{i,m+1} = k_{i,m} + w, \tag{5}$$

$$\mu_{i,m+1} = \frac{k_{i,m}\mu_{i,m} + wx_i}{k_{i,m}+w}, \tag{6}$$

$$\sigma^2_{i,m+1} = \sigma^2_{i,m} + \frac{k_{i,m}w}{k_{i,m}+w}(x_i - \mu_{i,m})^2. \tag{7}$$

Note that $n_{i,m}$ and $k_{i,m}$ have the same update, so one value can be stored to cover both, for all i. Given the above parameters, updated with the available evidence, a Gaussian may be drawn, to sample the probability of a colour being drawn from this mixture component.

Instead of drawing it the Gaussian is integrated out, to give

$$x_i \sim \mathcal{T}\left(n_{i,m}, \mu_{i,m}, \frac{k_{i,m}+1}{k_{i,m}n_{i,m}}\sigma^2_{i,m}\right), \tag{8}$$

where $\mathcal{T}(v, \mu, \sigma^2)$ denotes the three parameter student-t distribution. Consequentially each mixture component is actually a student-t distribution, to avoid the problem of sampling the Gaussian distribution that is actually being represented.

Background probability: The Chinese restaurant process is used to calculate the probability of a pixel, $\mathbf{x} \in [0,1]^3$ belonging to the background (bg) model. It integrates out the stick weights, unlike the stick breaking construction, which is essential to obtaining good performance. The probability of $\mathbf{x}$ given component (table) $t \in T$ is

$$P(\mathbf{x}|t, \text{bg}) = \frac{s_t}{\sum_{i \in T} s_i} P(x|n_t, k_t, \mu_t, \sigma^2_t), \tag{9}$$

$$P(\mathbf{x}|n_t, k_t, \mu_t, \sigma^2_t) = \prod_{i \in \{0,1,2\}} \mathcal{T}\left(x_i | n_{t,i}, \mu_{t,i}, \frac{k_{t,i}+1}{k_{t,i}n_{t,i}}\sigma^2_{t,i}\right), \tag{10}$$

where s_t is the number of samples assigned to component t, and n_t, μ_t, k_t and σ_t are the parameters of the prior updated with the samples currently assigned to the component. Note that s_t is the offset from the prior values for n_t and k_t, so these latter two do not need to be stored. By including a dummy component, $t = new \in T$, which represents creating a new component (sitting at a new table) with $s_{new} = \alpha$, this is the Chinese restaurant process. The student-t parameters for this dummy component are the prior without update. Finally, the mixture components can be summed out

$$P(\mathbf{x}|\text{bg}) = \sum_{t \in T} P(\mathbf{x}|t, \text{bg}). \tag{11}$$

The goal is to calculate $P(\text{bg}|\mathbf{x})$, not $P(\mathbf{x}|\text{bg})$, hence Bayes rule is applied,

$$P(\text{bg}|\mathbf{x}) = \frac{P(\mathbf{x}|\text{bg})P(\text{bg})}{P(\mathbf{x}|\text{bg}) + P(\mathbf{x}|\text{fg})}. \tag{12}$$

Note that pixels can only belong to either the background or the foreground (fg), hence the denominator. $P(\mathbf{x}|\text{bg})$ is given above, leaving $P(\text{bg})$ and $P(\mathbf{x}|\text{fg})$. $P(\text{bg})$ is an implicit threshold on what is considered background and what is considered foreground, and is thus considered to be a parameter. $P(\mathbf{x}|\text{fg})$ is unknown and hard to estimate, so the uniform distribution is used, which is a value of 1, as the volume of the colour space is 1 (see supplementary material).

Model update: To update the model at each pixel the current value is assigned to a mixture component, which is then updated - s_t is increased and the posterior for the Gaussian updated with the new evidence (Equations 4 - 7). Assignment is done probabilistically, by randomly drawing a component, weighted by $P(\mathbf{x}|t, \text{bg})$ (Equation 9). The possibility of assignment to a new mixture component is included - in the context of background subtraction this is the possibility that the pixel represents something we have not seen before. This is equivalent to Gibbs sampling the density estimate, except we only sample each value once, on arrival. In consequence samples do not need to be stored. Updates are weighted by their probability of belonging to the background (Equation 12), i.e. w is set to $P(\text{bg}|\mathbf{x})$ in Equations 4-7, and s_t is incremented by $P(\text{bg}|\mathbf{x})$. Sampling each value just once is not an issue, as the continuous stream of data combined with confidence capping means the model soon converges.

Confidence capping: A learning rate is not used; instead, unique to a DP-GMM, we introduce the notion of capping the confidence of the model. This can be interpreted as an adaptive update [9], [26], but it is both principled and very effective. In effect we are building an online density estimate with the ability to selectively forget, allowing newer data to take over when the background changes. If this was not done the model would get more confident as time goes on - if it had seen the background in its current state for 3 days then it would require 3 days of data showing the background in a different state before the new model became dominant. Confidence capping effectively limits the confidence so that a new model can always replace the old one in a short amount of time; it also avoids numerical overflow and allows single-sample Gibbs sampling to converge. The cap is applied to the largest individual component, rather than the distribution as a whole - this avoids mixtures with more components being required to use wider distributions to compensate.

Mathematically it works by capping how high s_t can go. When the cap is exceeded by any s_t for a pixel then a multiplier is applied to all s_t, scaling the highest s_t down to equal the cap. Note that s_t is tied to n_t and k_t, so they are also adjusted. As σ^2_t is dependent on k_t (it includes k_t as a multiplier) an update is avoided by storing σ^2_t/k_t instead. The effectiveness is such that it can learn the initial model with less than 30 frames of data yet objects can remain still for many minutes before being merged into the background. This does not impede the ability of the model to update as the background changes. Finally, in the limit as an infinite number of frames arrives the Dirichlet process will have an infinite number of components. This will exhaust a computer's memory; therefore the component count is also capped. When a new component is created the existing component with the lowest s_t is replaced.

2.2 Probabilistic Regularisation

The per-pixel background model ignores information from the neighbourhood of a pixel, leaving it susceptible to locally occurring noise and camouflage. Additionally, Gibbs sampling introduces a certain amount of noise, meaning that the boundary between foreground and background is subject to a dithering effect. To resolve these issues a Markov random field is constructed, with a node for each pixel, connected using a 4-way neighbourhood. It is a binary labelling problem, where each pixel either belongs to the foreground or to the background.

The task is to select the most probable solution, where the probability can be separated into two terms. Firstly, each pixel has a probability of belonging to the background or foreground (data term), directly obtained from the model as $P(\text{bg}|\mathbf{x})$ and $1 - P(\text{bg}|\mathbf{x})$, respectively. Secondly, there is the probability of being the same (smoothing term), which indicates how likely adjacent pixels have the same assignment,

$$P(l_a = l_b) = \frac{h}{h + m * \text{d}(a, b)}, \tag{13}$$

where l_y is the label of pixel y, h is a parameter that sets the half life, i.e. the distance at which the probability becomes 0.5, and $\text{d}(a, b)$ is the Euclidean distance between the two pixels in colour space. Noise suppression is greatly improved if at least one of the neighbours of a pixel have a high probability of being assigned the same label - this is the purpose of m. m is typically 1, but is decreased if a pixel is sufficiently far from its neighbours that none provides a $P(l(a) = l(b))$ value above a threshold. The decrease is such that at least one of them matches the threshold.

Various methods can be considered for solving this model. Graph cuts [38] would give the MAP solution, however we use loopy belief propagation instead [30], as it runs in constant time given an iteration cap, which is important for a real time implementation; it also runs considerably better on a GPU. A red-black [30] update schedule is used to save memory - a checkerboard pattern is assigned to the pixels and then all pixels of one colour send their messages, followed by all pixels of the other colour, and so on, until convergence. This results in half the memory consumption, as only messages going in one direction need to be stored; it additionally accelerates convergence [30]. Furthermore, a hierarchical implementation is used, whereby the model is first solved at a low resolution, before being scaled up, such that the transferred messages accelerate convergence at the higher resolution. This occurs over multiple levels - the number is decided by halving the resolution of the frame until either dimension drops below 32.

2.3 GPU Implementation

A background subtraction algorithm will have limited practical use if it cannot be run in real time on a video feed as it arrives. Accordingly, a GPU based implementation has been constructed. Because we have selected a naturally parallel structure for the presented approach adapting it to run on a GPU is relativity straightforward - the model for each pixel is independent, whilst regularisation with belief propagation can be implemented via message passing. The following phases exist:

1) Calculate the probability of the current pixel being drawn from each mixture component in the model, and also the new component probability. These computations are all independent.
2) Pull the probabilities together, to generate the probability of each pixel coming from the current model. Update the model using Gibbs sampling - random number generation is handled via the Philox algorithm [39]. This is independent on a per pixel basis.
3) Calculate the costs for belief propagation - this is naturally parallel.
4) Do message passing, over multiple hierarchical levels. The use of a red-black update schedule means that we can update half the pixels at each given step.
5) Extract the final mask - an independent calculation for each pixel.

Some approximations are made in the calculations to accelerate run time - these are detailed in the supplementary material.

Using the GPU implementation with a GeForce GTX 580 on a standard PC platform with a 4.4Ghz CPU, it can obtain 28.5 frames per second on input that has a resolution of 320×240 (Calculated for the problem cd-baseline-highway - see Section 3). Note that only 41% of the time is spent doing the background subtraction - another 19% is expended on colour conversion whilst 25% is spent estimating the lighting change, with the remainder on input/output. Neither colour conversation nor lighting change estimation were run on the GPU, and all processing occurs in sequence without any parallelism between the CPU and GPU.

2.4 Further Details

The core algorithmic details have now been given, but other pertinent details remain.

The prior: The background model includes a prior on the Gaussian associated with each mixture component. Instead of treating this as a parameter to be set, it is learnt from the data. Specifically, the mean and standard deviation (SD) of the prior are matched with the mean and SD of the pixels in the current frame, with the weight set so it is equivalent to a single sample,

$$n_{i,0} = k_{i,0} = 1, \qquad \mu_{i,0} = \frac{1}{|F|} \sum_{x \in F} x_i, \tag{14}$$

$$\sigma^2_{i,0} = \frac{1}{|F|} \sum_{x \in F} (x_i - \mu_{i,0})^2, \tag{15}$$

where F is the set of pixels in the current frame. To change the prior between frames the posterior parameters must not be stored directly, instead offsets from the prior are stored, which are then adjusted after each update such that the model is equivalent.

Illumination change: The above helps by updating the prior, but it does nothing to update the evidence. To update the evidence a multiplicative model is used,

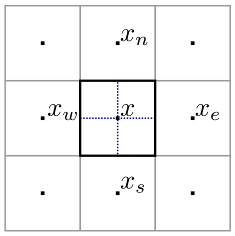

Fig. 3. Geometry of the interpolation used to handle camera shake. Each black dot is the centre of a pixel, for which we know a value - the five values used are labelled, with the compass directions. The standard deviation is calculated for the region inside the black square.

whereby the lighting change between frames is estimated as a multiplier, then the entire model is updated by multiplying the means, $\mu_{i,m}$, of the components accordingly. Light level change is estimated as in Loy et al. [40]. This takes every pixel in the frame and divides its value by the same pixel in the previous frame, as an estimate of the lighting change. The mode of these estimates is then found using mean shift [41], which is robust to the many outliers.

Robustness to Shadows: Shadows are typically of no interest to further processing, and hence should be ignored by background subtraction. A simple approach is to ignore luminance information [6], as this is the only channel in which (white light) shadows appear, but this throws away too much information. Instead a novel step is taken which involves reducing the importance of luminance, such that a wider range of brightness levels are accepted as belonging to the background. Luminance remains available for modelling by the background model. This is achieved with a new shadow-insensitive colour model - it is detailed in the supplementary material. It allows the approach to classify softer shadows as belonging to the background, but proves ineffective for hard/deep shadows.

Camera Shake: With few exceptions [42], [43] background subtraction algorithms assume a fixed camera. In practise even fixed cameras shake due to vibrations in their mounting structure, which can be caused, for instance, by the wind or passing traffic. To improve vibration handling when updating the model we use a region around each pixel, rather than the pixel value directly. Going back to Equation 7 it updates the model assuming a single point value - it can be modified to accept a Gaussian distribution instead, to get

$$\sigma^2_{i,m+1} = \sigma^2_{i,m} + w\varsigma^2_{i,m} + \frac{k_{i,m}w}{k_{i,m}+w}(x_i - \mu_{i,m})^2. \quad (16)$$

where ς is the standard deviation of the measured pixel value. Effectively it can be interpreted as the colour variance in the region around the pixel, from which we can randomly sample due to camera shake.

Assuming linear interpolation between adjacent values allows us to calculate the standard deviation of an image region, which we do for a single 1×1 pixel region around the point sampled. If we treat the image surface as being made of square regions rather than triangular regions we only need the values of three corners for each square, which halves the number of pixels that need to be fetched. Using Figure 3 the region being calculated is given by the black square, which is split into four sub-squares. Three corners of the top right sub-square are given by x, $h_n = \frac{x+x_n}{2}$ and $h_e = \frac{x+x_e}{2}$; the same pattern applies to the other three. The standard deviation of these four squares is hence given by

$$\begin{aligned}\varsigma = &\frac{x^2 + h_n^2 + h_e^2 + h_s^2 + h_w^2}{6} \\ &+ \frac{h_n h_e + h_e h_s + h_s h_w + h_w h_n}{8} \\ &+ \frac{x h_n + x h_e + x h_s + x h_w}{12} - \mu^2 \end{aligned} \quad (17)$$

where μ is the mean of the four squares, given by $\mu = \frac{h_n+h_e+h_s+h_w}{4}$. This has to be done for each of the three colour channels. As a further detail we scale the standard deviation with a parameter - a value of zero indicates that there is no camera shake, whilst 1 indicates a camera shake of about 1 pixel across. This approach will not scale for large amount of shake, but proves effective for the small quantities introduced by vibrations from, for instance, passing traffic.

Bootstrapping: The algorithm learns continuously - it does not need a learning period and can update as the scene changes. However, during initialisation the algorithm is not confident, and assumes everything belongs to the background. This makes the algorithm appear to be bad at bootstrapping - to obtain good performance it is forced to be over-confident. This is the opposite of confidence capping, in that it increases the confidence to the cap by multiplication. It is only applied whilst calculating $P(\text{bg}|\text{x})$ however - the actual parameters are not updated. This bias term exists purely to make the algorithm overconfident during initial model training, because some of the tests in Section 3 require results immediately from the first frame. For real world usage this would be switched off.

3 Experiments

Four data sets are used for the experiments:

- *sabs* from Brutzer et al. [2]. This one is synthetic[4].
- *wallflower* from Toyama et al. [1][5].
- *star* from Li et al. [12][6].
- *change detection* (cd) from Goyette et al. [13]. This has an online chart which is actively updated[7].

We perform extensive experiments using these data sets, allowing us to compare against a large number of alternative approaches. Brief summaries of many of the

4. Online at http://www.vis.uni-stuttgart.de/index.php?id=sabs.
5. Can be downloaded from http://research.microsoft.com/en-us/um/people/jckrumm/WallFlower/TestImages.htm.
6. http://perception.i2r.a-star.edu.sg/bk_model/bk_index.html.
7. Data set and chart online at http://www.changedetection.net.

confidence cap	Equivalent to the learning rate in other approaches.	128
concentration	Concentration parameter for the DP - controls new mixture component creation.	0.01
min weight	Minimum weight for mixing in new samples, to accelerate learning time when the background changes.	0.0001
sd mult	Size of blurring kernel used to negate light camera shake.	0.6
component cap	Maximum number of components for each pixel.	8

TABLE 1
Descriptions of the parameters for the DP-GMM. The final column contains the values used for the *cd* data set.

approaches we compare against can be found in Table 1 in the supplementary material. Results for the *wallflower* data set are also available in the supplementary material, as are parameter sweeps to demonstrate that performance remains high regardless of parameters. Table 1 gives the approaches parameters.

3.1 SABS

Brutzer et al. [2] presented a synthetic evaluation of background subtraction algorithms, consisting of a 3D rendering of a road junction, traversed by both cars and people - see Figure 5. Despite being synthetic it simulates, fairly accurately, nine real world problems, and has the advantage of having ground truth for all frames. The nine real world problems are

- *basic*, a baseline test.
- *dynamic background*, which crops the area of analysis to be the area of a waving tree.
- *bootstrap*, which has no training period, such that a clean background plate is never seen.
- *darkening*, which simulates the sun setting.
- *light switch*, which has the street at night and a shop switching its light off then on again.
- *noisy night*, which is the scene at night with heavy noise.
- *camouflage*, where the cars and people have been coloured similarly to the background, so they blend in.
- *no camouflage*, same as camouflage, but with easy to see colours, for comparison.
- *H264*, which compresses the video heavily, to generate typical compression artefacts.

The f-measure is reported for the various approaches in Table 2, and is defined as the harmonic mean of the recall and precision.

$$\text{recall} = \frac{\text{tp}}{\text{tp} + \text{fn}}, \quad \text{precision} = \frac{\text{tp}}{\text{tp} + \text{fp}} \tag{18}$$

$$\text{f-measure} = 2\frac{\text{recall} \cdot \text{precision}}{\text{recall} + \text{precision}} \tag{19}$$

using *fp* as the number of false positives, *tn* as the number of true negatives etc.

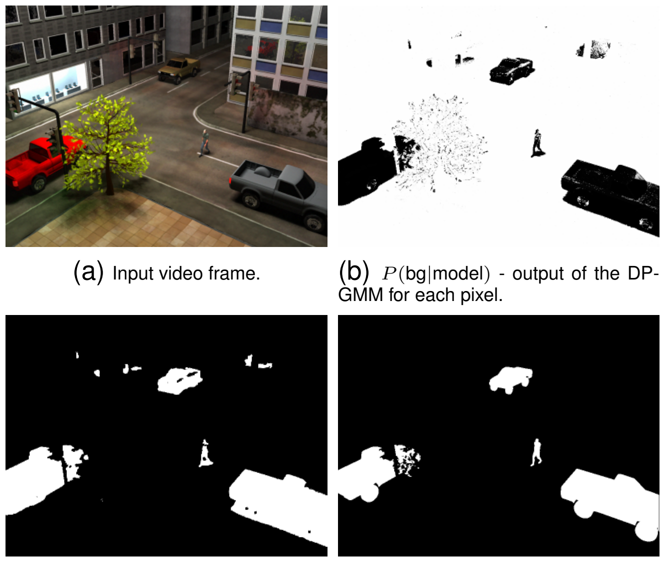
(a) Input video frame. (b) $P(\text{bg}|\text{model})$ - output of the DP-GMM for each pixel. (c) Foreground mask generated by the presented approach. (d) Ground truth foreground mask.

Fig. 5. Frame 545 from the bootstrap sequence of the SABS data set [2].

For this test we used one set of parameters for all scenarios, rather than tuning per problem[8]. As can be seen, the presented approach takes first place for all scenarios, and is on average 27% better than its nearest competitor. In doing so it demonstrates that it is not sensitive to the parameters chosen, as it can produce top results in many scenarios without per-problem tuning. Running without regularisation is also included in the chart (denoted as *DP, no post*)[9] - in all cases a lack of regularisation does not undermine its significant lead over the competition, demonstrating that the DP-GMM is doing most of the work, but that regularisation always improves the score, on average by 13%. It can be noted that the largest performance gaps between regularisation being off and being on appears for the noisiest inputs, e.g. noisy night, light switch, darkening and h264. These are the kinds of problems encountered in typical surveillance applications.

As a further point of comparison *DP, con com* is included, where our MRF-based post-processing has been swapped for the connected components method of Stauffer & Grimson [17]. Interestingly for the simpler problems it does very well, sometimes better than the presented method, but when it comes to the trickier scenarios the presented is clearly better. Figure 4 shows all the variants for a frame from noisy night. This demonstrates the key advantage of our post-processor - given a weak detection that falls below the implicit threshold it can convert it into a complete object, by

8. The test procedure allows tuning one parameter per test - we have thus put ourselves at a disadvantage.

9. The other algorithms on the chart have had their post-processing removed, so it can be argued that this is the fairer comparison to make, though Brutzer et al. [2] define post-processing such that our regularisation method is allowed.

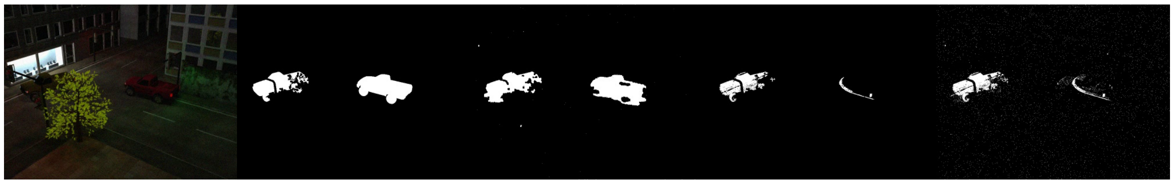

Fig. 4. Frame 990 from the noisy night sequence.

method	basic	dynamic background	bootstrap	darkening	light switch	noisy night	camouflage	no camouflage	h.264, 40kbps	*mean*
Stauffer [17]	.800 (3)	.704 (5)	.642 (5)	.404 (7)	.217 (6)	.194 (6)	.802 (4)	.826 (4)	.761 (6)	.594 (7)
Maddalena [19]	.766 (5)	.715 (3)	.495 (7)	.663 (5)	.213 (7)	.263 (5)	.793 (5)	.811 (5)	.772 (5)	.610 (6)
Li 1 [18]	.766 (5)	.641 (6)	.678 (4)	.704 (3)	.316 (3)	.047 (7)	.768 (6)	.803 (6)	.773 (4)	.611 (5)
Barnich [8]	.761 (6)	.711 (4)	.685 (3)	.678 (4)	.268 (5)	.271 (4)	.741 (7)	.799 (7)	.774 (3)	.632 (4)
Zivkovic [9]	.768 (4)	.704 (5)	.632 (6)	.620 (6)	.300 (4)	.321 (3)	.820 (3)	.829 (3)	.748 (7)	.638 (3)
DP-GMM, no post	.836 (2)	.827 (2)	.717 (2)	.736 (2)	.499 (2)	.346 (2)	.848 (2)	.851 (2)	.781 (2)	.715 (2)
DP-GMM	**.853** (1)	**.853** (1)	**.796** (1)	**.861** (1)	**.603** (1)	**.788** (1)	**.864** (1)	**.867** (1)	**.827** (1)	**.812** (1)
DP-GMM, con com	.855	.872	.722	.818	.500	.393	.847	.851	.838	.744

TABLE 2
SABS [2] results: F-measures for each of the 9 challenges. The results for other algorithms were obtained from the website (As of Feb 2013), though algorithms that never got a top score in the original chart have been omitted. Algorithm rank is given by the numbers in brackets. The mean column gives the average for all tests - the presented approach is 27% higher than its nearest competitor.

utilising both colour consistency and model uncertainty.

The frame shown in Figure 5 has been chosen to demonstrate two areas in which the algorithm performs poorly. Specifically, its robustness to shadows is not very effective - whilst this could be improved by reducing the importance of luminance in the colour space this has the effect of reducing its overall ability to distinguish between colours, and undermines performance elsewhere. The second issue can be seen in the small blobs at the top of the image - they are actually the reflections of cars and people in the scene. Using a DP-GMM allows it to learn a very precise model, so much so that it can detect the slight deviation caused by a reflection, when it would be preferable to ignore it. Further processing could potentially avoid this.

3.2 Star

The *star* data set [12] is very similar to the *wallflower* data set - *bootstrap* from *wallflower* is the same video as *br* in this data set. To its advantage *star* has an improved testing procedure however, as it provides multiple test frames per problem, with performance measured using the average similarity score for all test frames, where similarity $= \text{tp}/(\text{tp}+\text{fn}+\text{fp})$. In addition the sequences are generally much harder, due to text overlays, systemic noise and some camera shake. Fewer algorithms have been run on it. The presented approach[10] takes 1^{st} 7 times out of 9, beaten twice by Maddalena et al. [19], though in both cases by a small margin. The light switch test in this data set does not trip it up this time - the library where it occurs has a high ceiling and diffuse lighting, making multiplicative lighting much more reasonable. Complex dynamic backgrounds clearly demonstrate the strength of a DP-GMM, as evidenced by its three largest improvements (*cam*, *ft* and *ws*).

3.3 Change Detection (cd)

The change detection [13] data set is much larger than any of the others, and includes a dense ground truth - masks are provided for all frames past some initial training period. It additionally limits parameter tuning such that a single parameter set must be used for all 31 videos. Video resolution is not great however, and many of the videos are of dubious quality; many appear to have been post-processed, often with a low quality deinterlacing algorithm that leaves ghosts[11]The videos are divided into six categories, which can be seen alongside the results in Figure 7. Quantitative results can be found in Table 4[12]. The online version considers many different scoring mechanism, and then combines them in a non-linear rank based system[13]. Instead we present the f-measure scores only, as it is the most used metric.

We now consider each test in turn.

- *Baseline*. A basic set of videos, with nothing unusual, though *pedestrians* has saturated colour. All the top algorithms get comparable scores for this test.

10. We tune per-problem, as all the competitors have done the same. Results for a single set of parameters are also presented.

11. From Figure 7 the *traffic* video demonstrates ghosting; the *abandoned box* video is an example of another kind of defect. It should be noticed that the other real data sets have similar issues.

12. The table is accurate as of February 2013 - an up to date version can be found at http://changedetection.net

13. This is problematic - the addition of a new approach can cause two unrelated algorithms to switch places. This can even occur when the new algorithm is much better or worse than those it reorders.

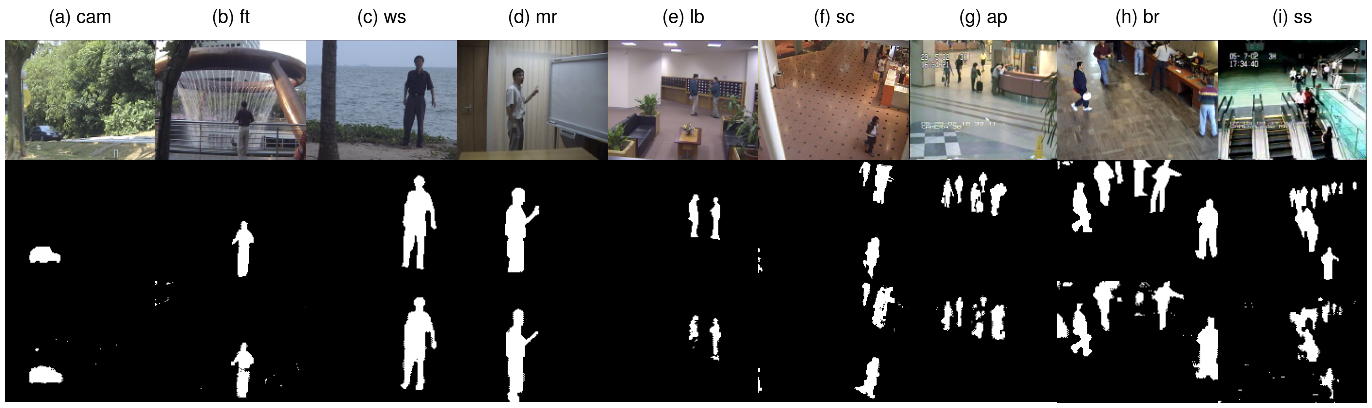

Fig. 6. *Star* results: On the top row is the image, on the second row the ground truth and on the third row the output of the presented algorithm. We use the same frames as Culibrk et al. [44] and Maddalena & Petrosino [19], for a qualitative comparison. The videos are named using abbreviations of their locations.

method	cam	ft	ws	mr	lb	sc	ap	br	ss	*mean*
Li 2 [12]	.1596 (5)	.0999 (6)	.0667 (6)	.1841 (6)	.1554 (6)	.5209 (6)	.1135 (6)	.3079 (6)	.1294 (6)	.1930 (6)
Stauffer [17]	.0757 (6)	.6854 (3)	.7948 (4)	.7580 (4)	.6519 (2)	.5363 (5)	.3335 (5)	.3838 (5)	.1388 (5)	.4842 (5)
Culibrk [44]	.5256 (4)	.4636 (5)	.7540 (5)	.7368 (5)	.6276 (4)	.5696 (4)	.3923 (4)	.4779 (4)	.4928 (4)	.5600 (4)
Maddalena [19]	.6960 (3)	.6554 (4)	.8247 (3)	.8178 (3)	.6489 (3)	.6677 (2)	**.5943** (1)	.6019 (3)	**.5770** (1)	.6760 (2)
DP-GMM	.7567 (2)	.7049 (2)	.9090 (2)	.8203 (2)	.5794 (5)	.6522 (3)	.5484 (3)	.6024 (2)	.5055 (3)	.6754 (3)
DP-GMM, tuned	**.7876** (1)	**.7424** (1)	**.9298** (1)	**.8411** (1)	**.6665** (1)	**.6733** (1)	.5675 (2)	**.6496** (1)	.5522 (2)	**.7122** (1)

TABLE 3
Star [12], [19] results: Refer to Figure 6 for exemplar frames, noting that *lb* has abrupt lighting changes. The average improvement of *DP, tuned* over its nearest competitor is 5%.

task	Baseline	Dynamic Background	Camera Jitter	Intermittent Motion	Shadow	Thermal	*mean*
Chebyshev [35]	-	.7656 (2)	-	-	.8333 (3)	.7259 (6)	-
KDE - ElGammal [6]	.9092 (8)	.5961 (18)	.5720 (16)	.4088 (20)	.8028 (7)	.7423 (3)	.6719 (11)
Chebyshev + static [35]	.8646 (12)	.7520 (3)	.6416 (12)	.3863 (23)	.8333 (4)	.7230 (7)	.7001 (9)
SGMM [45]	.8594 (13)	.6380 (14)	.7251 (4)	.5397 (10)	.7617 (8)	.6481 (18)	.7008 (8)
SOBS [20]	.9251 (4)	.6439 (12)	.7086 (8)	.5628 (7)	.7716 (11)	.6834 (14)	.7159 (7)
CDPS [46]	.9208 (7)	.7495 (4)	.4865 (21)	**.7406** (1)	.8092 (6)	.6619 (16)	.7281 (6)
SC-SOBS [21]	**.9333** (1)	.6686 (10)	.7051 (9)	.5918 (4)	.7786 (10)	.6923 (13)	.7283 (5)
PSP-MRF [29]	.9289 (2)	.6960 (5)	.7502 (2)	.5645 (6)	.7907 (9)	.6932 (12)	.7372 (4)
PBAS [10]	.9242 (5)	.6829 (7)	.7220 (5)	.5745 (5)	.8597 (2)	.7556 (2)	.7532 (3)
SGMM-SOD [47]	.9223 (6)	.6826 (8)	.7000 (10)	.6957 (2)	**.8659** (1)	.7081 (8)	.7624 (2)
pROST [25]	.799 (22)	.595 (21)	**.792** (1)	.419 (21)	.706 (23)	.584 (23)	.650 (16)
DP-GMM	.9286 (3)	**.8137** (1)	.7477 (3)	.5418 (9)	.8127 (5)	**.8134** (1)	**.7763** (1)

TABLE 4
CD [13] results: This chart only contains the most competitive algorithms - the online chart includes many more. The rank after each f-measure takes into account the omitted approaches. Refer to Figure 7 for example frames.

- *Dynamic Background*. These videos have complex multi-modal backgrounds, such as water. As demonstrated previously, the presented excels at such input, outperforming the competitors significantly.
- *Camera Jitter*. The camera is not properly mounted for these videos, and as such shakes. This does reduce the quality of our output - the output frames tend to miss parts of objects due to the wider background model induced by the shaking. It also incorrectly classifies the background during the worst shakes, but we still manage a close second place.
- *Intermittent Motion*. This involves objects being left alone (static), and is our weakest result. Other approaches often have a specific code path to handle this situation, whilst we do not, putting us at a disadvantage.
- *Shadow*. These videos have shadows, and test the ability of the approach to ignore them. In our case we have some capability to handle soft shadows, as seen in *cubicle*, but will typically detect hard shadow regions. Interestingly our result remains among the top approaches despite its limited capabilities.
- *Thermal*. A somewhat unusual video source, this demonstrates cameras for low light recording. Such sources have a large amount of noise, which the presented is expected to do well on. Unsurprisingly it demonstrates a strong lead over the competition. It actually suffers from being too sensitive - in *corridor* it detects the thermal reflections when these

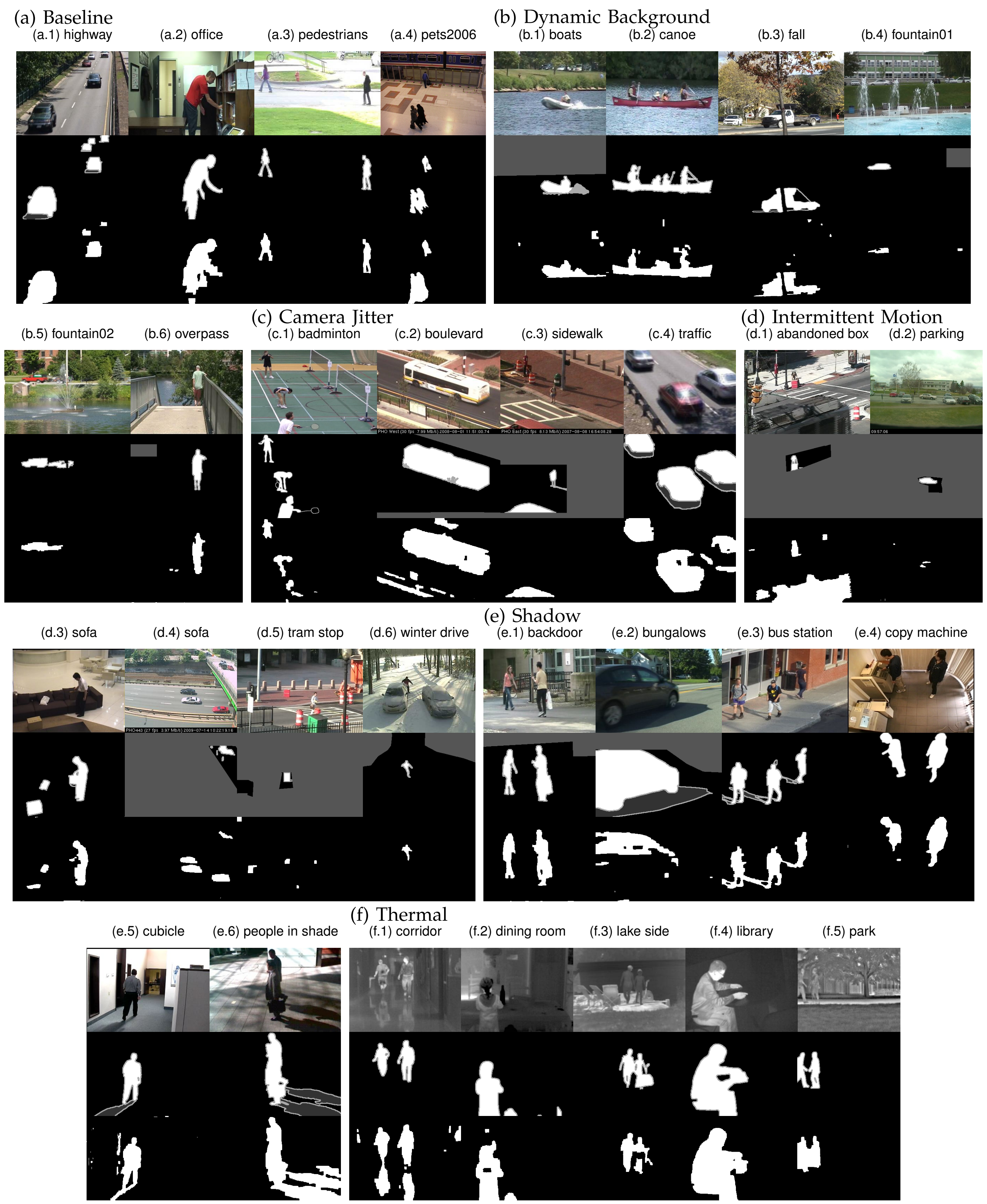

Fig. 7. *CD* results: Layout is identical to Figure 6, with multiple rows. The ground truth includes various shades of grey - a dark grey to indicate shadowed regions, a mid grey for areas that are ignored when scoring for all frames and a light grey for areas ignored for just this frame. Mid grey is used to focus on the action being tested, whilst light grey indicates areas where foreground/background assignment is ambiguous (typically presents as a thin line around each segment).

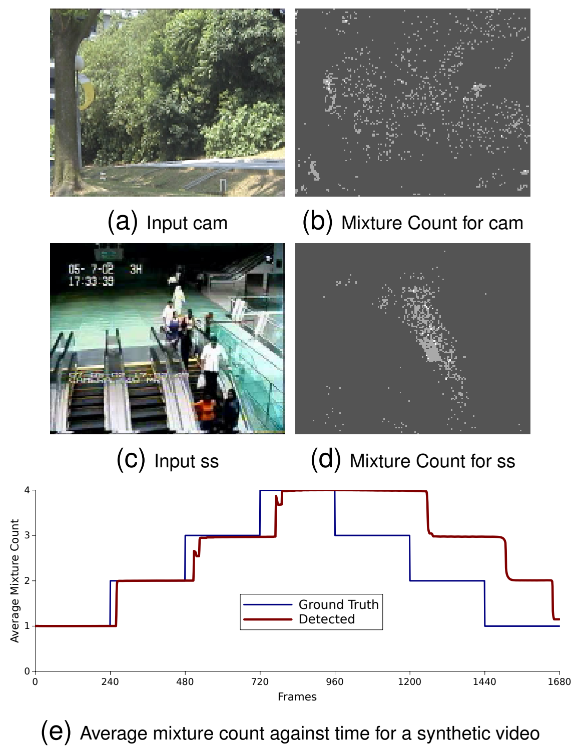

Fig. 8. Representations of the per-pixel mixture count - see text for details.

should be considered background.

Overall we win on average for the *cd* data set (Table 4). This is because the DP-GMM model can handle backgrounds that are complex and dynamic, due to its ability to estimate mixture components automatically and avoid over-/under- fitting. This ability, in combination with the regularisation based on a Markov random field allows it to effectively cope with heavy noise.

3.4 Mixture Count

The approach implicitly calculates a mixture count for each pixel[14] - Figure 8 visualises this. (a) - (d) show two frames from the *star* data set, and their corresponding per pixel mixture counts for the thousandth frame. The images are coloured such that black is 0 components and white is 4 - the majority of pixels in both frames have been estimated to have 1 component. Trees moving in *cam* create components where the movement is large, though note that most areas can be handled using a single wide variance component. In *ss* the escalators again generate extra components, though being mostly black they can often be covered by a single component. The heavily used escalator on the right gets lots of components because the approach forms one for the people going past, in case they stop and become part of the background. These components are never considered to be part of the background as they don't obtain enough weight. (e) demonstrates the mixture count changing over time, with a synthetic video. The video shows 10 seconds of 1 mode, then 2 modes, and so on up to 4, then back again, at 24 fps - the ground truth mode count is plotted[15]. We can plot the mode count, averaged over all the pixels - it follows ground truth, with lag as expected. Note that the lag is very short when learning a new mixture component - only about 2 seconds, but very slow when it comes to forgetting a background component, which is desirable.

4 Conclusions

We have presented a new background subtraction method and validated its effectiveness with extensive testing. The method is based on an existing model, namely DP-GMMs, but with new model learning algorithms developed to make it both suitable for background modelling, and computationally scalable. Whilst the basic concept of per-pixel density estimate (DE) can be traced back to Stauffer & Grimson [17], the use of a non-parametric Bayesian model gives it a significant advantage when it comes to handling dynamic backgrounds. Specifically, our model is able to learn the number of mixture components more accurately and hence better cope with a variety of scene changes, in comparison with the existing more heuristic DE methods. It also proves itself to have good performance in many other areas, particularly on dealing with heavy noise. Despite its thorough theoretical basis implementation remains relatively simple[16].

A number of improvements can be considered. Combining information between pixels only as a regularisation step does not fully exploit the information available. A more rigorous method of spatial information transmission would be desirable - a dependent Dirichlet process could provide this. Sudden complex lighting changes are not handled, which means it fails to handle some indoor lighting changes. Furthermore, a more sophisticated model of the foreground and an explicit model of left objects could further improve our method. Solutions to these problems from many of the existing methods could be adapted to ours [6], [33], [35].

References

[1] K. Toyama, J. Krumm, B. Brumitt, and B. Meyers, "Wallflower: Principles and practise of background maintenance," *ICCV*, pp. 255–261, 1999.

[2] S. Brutzer, B. Hferlin, and G. Heidemann, "Evaluation of background subtraction techniques for video surveillance," *CVPR*, 2011.

[3] M. D. Escobar and M. West, "Bayesian density estimation and inference using mixtures," *J. American Statistical Association*, vol. 90(430), pp. 577–588, 1995.

14. Because it is using a DPMM the mixture count is principally always infinity, but a reasonable approximation can be obtained using a threshold.

15. The video changes colour repeatedly, cycling though all modes every second and showing each for an equal amount of time. It includes noise.

16. 186 lines of C for the DP model and 239 lines for the post-processing. The GPU implementation comes in at 814 lines, due to the complex processing structure needed for an efficient implementation.

[4] Y. W. Teh and M. I. Jordan, *Bayesian Nonparametrics*. Cambridge University Press, 2010, ch. Hierarchical Bayesian Nonparametric Models with Applications.

[5] Y. He, D. Wang, and M. Zhu, "Background subtraction based on nonparametric bayesian estimation," *Int. Conf. Digital Image Processing*, 2011.

[6] A. Elgammal, D. Harwood, and L. Davis, "Non-parametric model for background subtraction," *Frame-rate Workshop*, pp. 751–767, 2000.

[7] Y. Sheikh and M. Shah, "Bayesian modeling of dynamic scenes for object detection," *PAMI*, vol. 27(11), pp. 1778–1792, 2005.

[8] O. Barnich and M. V. Droogenbroeck, "Vibe: A powerful random technique to estimate the background in video sequences," *Acoustics, Speech and Signal Processing*, pp. 945 – 948, 2009.

[9] Z. Zivkovica and F. Heijden, "Efficient adaptive density estimation per image pixel for the task of background subtraction," *Pattern Recognition Letters*, pp. 773–780, 2006.

[10] M. Hofmann, P. Tiefenbacher, and G. Rigoll, "Background segmentation with feedback: The pixel-based adaptive segmenter," *Workshop on Change Detection, CVPR*, pp. 38–43, 2012.

[11] T. S. F. Haines and T. Xiang, "Background subtraction with dirichlet processes," *ECCV*, 2012.

[12] L. Li, W. Huang, I. Y.-H. Gu, and Q. Tian, "Statistical modeling of complex backgrounds for foreground object detection," *IEEE Tran. IP*, vol. 13(11), pp. 1459–1472, 2004.

[13] N. Goyette, P.-M. Jodoin, F. Porikli, J. Konrad, and P. Ishwar, "changedetection.net: A new change detection benchmark dataset," *Workshop on Change Detection, CVPR*, pp. 16–21, 2012.

[14] S.-C. S. Cheung and C. Kamath, "Robust techniques for background subtraction in urban traffic video," *VCIP*, vol. 5308, pp. 881–892, 2004.

[15] M. Karaman, L. Goldmann, D. Yu, and T. Sikora, "Comparison of static background segmentation methods," *VCIP*, vol. 5960, pp. 2140–2151, 2005.

[16] S. Herrero and J. Bescos, "Background subtraction techniques: Systematic evaluation and comparative analysis," *ACIVS*, pp. 33–42, 2009.

[17] C. Stauffer and W. E. L. Grimson, "Adaptive background mixture models for real-time tracking," *CVPR*, vol. 2, pp. 637–663, 1999.

[18] L. Li, W. Huang, I. Y. H. Gu, and Q. Tian, "Foreground object detection from videos containing complex background," *Proc. Multimedia*, pp. 2–10, 2003.

[19] L. Maddalena and A. Petrosino, "A self-organizing approach to background subtraction for visual surveillance applications," *IEEE Tran. IP*, vol. 17(7), pp. 1168–1177, 2008.

[20] ——, "A fuzzy spatial coherence-based approach to background/-foreground separation for moving object detection," *Neural Computing and Applications*, vol. 19(2), pp. 179–186, 2010.

[21] ——, "The sobs algorithm: what are the limits?" *Workshop on Change Detection, CVPR*, pp. 21–26, 2012.

[22] J. Kato, T. Watanabe, S. Joga, J. Rittscher, and A. Blake, "An hmm-based segmentation method for traffic monitoring movies," *PAMI*, vol. 24(9), pp. 1291–1296, 2002.

[23] N. Oliver, B. Rosario, and A. P. Pentland, "A bayesian computer vision system for modeling human interactions," *PAMI*, vol. 22(8), pp. 831–843, 2000.

[24] J. He, L. Balzano, and A. Szlam, "Incremental gradient on the grassmannian for online foreground and background separation in subsampled video," *CVPR*, 2012.

[25] F. Seidel, C. Hage, and M. Kleinsteuber, "prost : A smoothed lp-norm robust online subspace tracking method for realtime background subtraction in video," *Unpublished, preprint in CoRR*.

[26] D.-S. Lee, "Effective gaussian mixture learning for video background subtraction," *PAMI*, vol. 27(5), pp. 827–832, 2005.

[27] K. Kim, T. H. Chalidabhongse, D. Harwood, and L. Davis, "Background modeling and subtraction by codebook construction," *ICIP*, vol. 5, pp. 3061–3064, 2004.

[28] J. Migdal and W. E. L. Grimson, "Background subtraction using markov thresholds," *Workshop on Motion and Video Computing*, pp. 58–65, 2005.

[29] A. Schick, M. Bauml, and R. Stiefelhagen, "Improving foreground segmentation with probabilistic superpixel markov random fields," *Workshop on Change Detection, CVPR*, pp. 27–31, 2012.

[30] P. F. Felzenszwalb and D. P. Huttenlocher, "Efficient belief propagation for early vision," *CVPR*, vol. 70(1), pp. 41–54, 2004.

[31] S. Cohen, "Background estimation as a labeling problem," *ICCV*, pp. 1034–1041, 2005.

[32] D. H. Parks and S. S. Fels, "Evaluation of background subtraction algorithms with post-processing," *Adv. Video and Signal Based Surveillance*, pp. 192–199, 2008.

[33] R. Cucchiara, C. Grana, M. Piccardi, and A. Prati, "Detecting moving objects, ghosts and shadows in video streams," *PAMI*, vol. 25(10), pp. 1337–1342, 2003.

[34] M. Harville, G. G. Gordon, and J. Woodfill, "Adaptive video background modeling using color and depth," *ICIP*, vol. 3, pp. 90–93, 2001.

[35] A. Morde, X. Ma, and S. Guler, "Learning a background model for change detection," *Workshop on Change Detection, CVPR*, pp. 15–20, 2012.

[36] D. M. Blei and M. I. Jordan, "Variational inference for dirichlet process mixtures," *Bayesian Analysis*, pp. 121–144, 2005.

[37] A. Gelman, J. B. Carlin, H. S. Stern, and D. B. Rubin, *Bayesian Data Analysis*. Chapman & Hall, 2004.

[38] Y. Boykov, O. Veksler, and R. Zabih, "Fast approximate energy minimization via graph cuts," *PAMI*, vol. 23, pp. 1222–1239, 2001.

[39] J. K. Salmon, M. A. Moraes, R. O. Dror, and D. E. Shaw, "Parallel random numbers: As easy as 1, 2, 3," *Int. Conf. High Performance Computing*, 2011.

[40] C. C. Loy, T. Xiang, and S. Gong, "Time-delayed correlation analysis for multi-camera activity understanding," *IJCV*, vol. 90(1), pp. 106–129, 2010.

[41] D. Comaniciu and P. Meer, "Mean shift: A robust approach toward feature space analysis," *PAMI*, vol. 24(5), pp. 603–619, 2002.

[42] X. Cui, J. Huang, S. Zhang, and D. Metaxas, "Background subtraction using group sparsity and low rank constraint," *ECCV*, 2012.

[43] A. Elqursh and A. Elgammal, "Online moving camera background subtraction," *ECCV*, 2012.

[44] D. Culibrk, O. Marques, D. Socek, H. Kalva, and B. Furht, "Neural network approach to background modeling for video object segmentation," *Neural Networks*, vol. 18(6), pp. 1614–1627, 2007.

[45] R. H. Evangelio, M. Ptzold, and T. Sikora, "Splitting gaussians in mixture models," *Advanced Video and Signal-Based Surveillance*, pp. 300–305, 2012.

[46] F. Hernandez-Lopez and M. Rivera, "Change detection by probabilistic segmentation from monocular view," *Submitted to Machine Vision and Applications*.

[47] R. H. Evangelio and T. Sikora, "Complementary background models for the detection of static and moving objects in crowded environments," *Adv. Video and Signal-Based Surveillance*, pp. 71–76, 2011.

Tom S.F. Haines received his PhD from the University of York in 2009 on shape from shading and stereopsis. Following this he did a post doctorate at Queen Mary, University of London, where he worked on topic models, active learning and background subtraction. He is now at University College London, doing research into handwriting. His interests include machine learning, non-parametric Bayesian methods, belief propagation and density estimation.

Tao Xiang received his PhD degree in electrical and computer engineering from the National University of Singapore in 2002. He is currently a Senior Lecturer (Associate Professor) in the School of Electronic Engineering and Computer Science, Queen Mary University of London. His research interests include computer vision, statistical learning, video processing, and machine learning, with a focus on interpreting and understanding human behaviour. He has published over 100 papers on international journals and conferences and coauthored a book Visual Analysis of Behaviour: From Pixels to Semantics.